Defect engineering using microwave processing in SiC and GaAs

Oleg Olikh[1]‡**, Petro Lytvyn**[2]

[1]Physics Faculty, Taras Shevchenko National University of Kyiv, Kyiv 01601, Ukraine
[2]V. Lashkaryov Institute of Semiconductor Physics of NAS of Ukraine, Kyiv 03028, Ukraine

E-mail: olegolikh@knu.ua

Abstract. The influence of microwave radiation (2.45 GHz, 1.5 W/cm^2, up to 80 s) on defects was studied in single crystals of n-6H–SiC, n-GaAs, and epi-GaAs. The capture cross section of the charge carrier was found to change, and defect complexes were reconstructed because of the growing number of interstitial atoms in the near-surface layer. The correlation between the changes in the defect subsystem and deformation of the near-surface layer was analyzed. The possible mechanisms of the revealed effects are also discussed.

Keywords: microwave, defect, SiC, GaAs

Submitted to: *Semicond. Sci. Technol.*

‡ Author to whom any correspondence should be addressed.

1. Introduction

Microelectronics is currently a field of primary importance, and the investigation of how semiconductors and their structural properties change under the action of various external factors has become one of the most important tasks in material science. Numerous theoretical and experimental studies have aimed to reveal the degradation mechanisms of semiconductor structures and to develop new technologies for microelectronic devices improvement. The influence of certain factors, for example, radiation, has been studied quite well — see, for instance, [1, 2, 3]. At the same time, new agents begin to attract more attention, such as ultrasound loading (USL) [4, 5], or microwave treatment (MWT) [6, 7, 8, 9, 10, 11, 12, 13, 14, 15, 16, 17, 18, 19]. The MWT has been widely applied owing to its capability of heating solid bodies [6, 7]. This approach is unique because of its high efficiency and capability to increase the temperature of a sample as a whole or at selected locations with extremely high heating speeds [6]. As a result, MWTs are widely used to synthesize various materials, and semiconductor compounds including [6, 8]. However, this type of external influence also causes changes in the characteristics of semiconductor materials and device structures. For instance, it has been found that irradiation by superhigh-frequency electromagnetic waves causes relaxation of internal stresses and modification of near-surface regions in GaAs and InP structures [11, 10, 12, 13, 15, 18, 19], leveling of surface microrelief in SiC/SiO_2 structures [9], redistribution of impurities [9, 16, 18], re–charge of complexes [12] and generation of defects [16]. The microwave-induced restructuring of impurity defects leads to a decrease in the spread of the Schottky diode parameters [12, 16]. Moreover, MWT has been found to induce changes in the properties of Ti, Gd, and Er films deposited on silicon carbide [17], as well as in the reconstruction of GaAs photoluminescence spectra [13, 15, 16], and the effect depends on both the type of dopant and the crystal structure orientation of the samples. Overall, these facts allow us to consider the MWT as one of the most promising ways to modify semiconductor devices.

However, it is well known that the properties of semiconductor structures are significally influenced by their defect subsystem. Defects in SiC and GaAs have been investigated extensively [20, 21, 22, 23]. At the same time, more detailed information regarding the MWT influence on the deep level parameters is practically unknown. The aim of this study was to investigate the impact of MWT on the defects located in the near-surface region of n–6H–SiC and n–GaAs single crystals, and GaAs epitaxial structures. The acoustoelectric transient spectroscopy was used to characterize the deep levels.

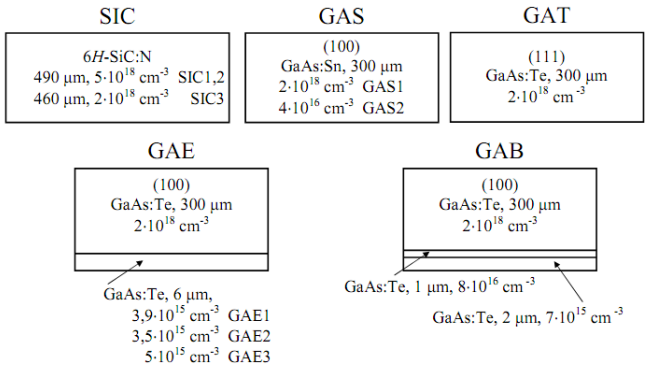

Figure 1. Schematic structure of the samples for deep level investigations

2. Experimental details

It has been reported [11, 12, 13, 14, 15] that the impact of MWT on semiconductor structures depends on many factors. The primary factors are the initial level of structural perfectness, conductivity, dielectric permittivity, and structural topology. To estimate the effect of MWT on the defect parameters, we selected different samples based on the doping degree, initial level of residual mechanical stress, and structure. They were as follows.

i) Single-crystal n–6H–SiC wafers were grown using the Leli method and were doped with nitrogen. The samples were 490 μm-thick plates with dimensions of 5×10 mm^2 and carrier concentration $(3-6)\times10^{18}$ cm^{-3} (further on SIC1 and SIC2); and 460 μm thick wafers with the same dimensions and carrier concentration $(1-3)\times10^{18}$ cm^{-3} (SIC3).

ii) GaAs single-crystal plates with a thickness of 300 μm. The plates were (100) oriented, doped with tin, and the concentration of electrons was $(1.5-2.5)\times10^{18}$ cm^{-3} for sample GAS1 and $(3-5)\times10^{16}$ cm^{-3} for sample GAS2. GAT denotation is used for wafer (111), which was doped by tellurium, $n=(1-2)\times10^{18}$ cm^{-3}.

iii) Epitaxial n-n^+ structures of GaAs which were 300 μm thick single crystal substrates $n=2\times10^{18}$ cm^{-3} covered with 6 μm thick layer with carrier concentration 3.9×10^{15} cm^{-3} (sample GAE1), 3.5×10^{15} cm^{-3} (GAE2), 5.0×10^{15} cm^{-3} (GAE3). The substrate and epitaxial layers were doped with Te.

iv) Epitaxial n-n^+-n^{++} structures of GaAs:Te with a buffer layer. They were made from a single-crystal (100) substrate (300 μm, $n=2\times10^{18}$ cm^{-3}) subsequently covered with a 1 μm layer with $n=8\times10^{16}$ cm^{-3} and a 2 μm layer with $n=7\times10^{15}$ cm^{-3}. Two samples (GAB1 and GAB) were cut from different wafers and were used in this study.

Epitaxial systems have been produced using gas-phase epitaxy. The samples used in the experiments are shown in figure 1.

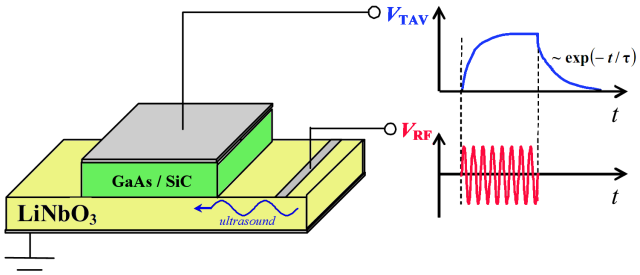

Figure 2. Scheme of TAV signal measurements. Time dependence of radio impulse V_{RF} of ultrasound excitation in piezoelectric plate and the resulting TAV signal V_{TAV} are shown schematically

The MWTs of the samples were performed in free space at room temperature in a magnetron at a frequency of $\nu = 2.45$ GHz and specific power of 1.5 W/cm^2. The epitaxial structures were irradiated onto the side of the epitaxial layer. The total exposure time t_{MWT} varied in the range of 20−80 s for the different samples. To avoid essential heating, the maximum single irradiation exposure time was no more than five seconds.

The parameters of deep centers, such as the efficient cross section of electron capture σ_n and location of the center energy level with respect to the conductivity band bottom $E_c - E_t$ were determined before and after MWT. For this purpose, we used acoustoelectric transient spectroscopy [24, 25, 26, 27]. A schematic representation of this method is shown in figure 2. The samples were placed on a $LiNbO_3$ piezoelectric plate in which acoustic waves were excited as impulses. After ultrasound impulse termination, relaxation of the transverse acoustoelectric voltage (TAV) occurs according to

$$V_{TAV}(t) = V_{TAV,0} \exp(-t/\tau). \quad (1)$$

A simple exponential dependence according to equation (1) is observed in cases where only one type of deep center is effective in acoustoelectric interactions. For n-type semiconductors, the characteristic relaxation time is described by the equation [24, 27]

$$\tau = \frac{1}{\sigma_n \upsilon_{th,n} N_c} \exp\left(\frac{E_c - E_t}{kT}\right), \quad (2)$$

where $\upsilon_{th,n}$ is the electron thermal velocity and N_c is the density of states in the conduction band.

The experimental measurements of the TAV relaxation at different temperatures and further approximation of the results according to equation (1) allowed us to obtain the $\tau(T)$ dependence. $E_c - E_t$ was determined from the slope of τ dependence on $(kT)^{-1}$ in semi-logarithmic scale and then, using equation (2), σ_n was calculated. The measurements were performed in the temperature range (290 − 350) K except for the GAB samples, the TAV for which was high enough to be measured only after heating to above 310 K.

For single–crystal samples before and after MWT, we also determined the curvature radius R_{cur} and deformation ξ_{cur} of the near-surface crystallographic planes. The value of ξ_{cur} was estimated by the X-ray method from the change in the angle of the diffraction maximum location during sample translation [28], and the curvature was measured using a profilometer DekTak 3030 Veeco Instruments. R_{cur} and ξ_{cur} were measured with a relative error no more than 2 %. For GaAs single crystals, we also analyzed the distribution of structural defects over the area using the Borman X-ray projection topography method, and estimated the distribution of dislocation densities and microstresses from the analysis of the intensities of the Friedel reflection pairs hkl and $hk\bar{l}$.

3. Results and discussion

Figure 3 presents the typical temperature dependencies of τ for the samples before and after the MWT. The above data show the change not only in the curve slopes (which is directly related to the level location in the gap), but also in the absolute value of the characteristic time of the relaxation TAV after MWT. The character of the MWT impact (the decrease or increase in relaxation time) depends not only on the exposure time and degree of doping but also on the internal structure of the samples under study. The results are presented in table 1. In the silicon carbide samples, there are two deep levels, labeled ESC1 and ESC2, while in gallium arsenide, there are six (EGA1–EGA6).

The presented data show a number of characteristic features:

i) The value of the carrier capture cross section is much more sensitive to the MWT than the energy location of the levels. For example, σ_n was found to change by an order of magnitude when the level location displacement was no more than 20%, and the capture cross section was modified at lower exposition times. For instance, the value of $(E_c - E_t)$ for GAB1 practically did not change after 20 s of MW exposure, whereas σ_n grew approximately four times.

ii) In single crystals, the MWT-induced changes become stronger as the free charge carrier concentration decreases (see data on samples GAS1 and GAS2) and the relative deformation increases (the increase in surface curvature).

iii) After durable MWT of single-crystal samples ($t_{MWT} > 40$ s for GaAs, $t_{MWT} > 80$ s for SiC), the TAV signal essentially decreased. This fact correlates with the data from [16], who reported a decrease in the concentration of centers with levels in the upper half of the band gap as a result of MW annealing.

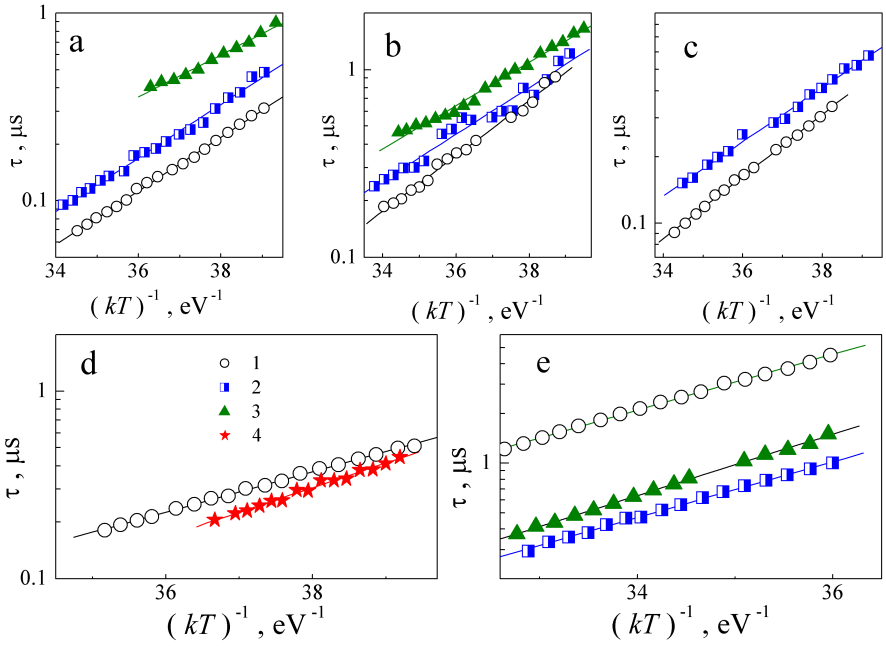

Figure 3. Dependences of TAV relaxation time on inverse temperature for samples SIC2 (a), SIC3 (b), GAS2 (c), GAE2 (d) and GAB1 (e) before and after MWT. t_{MWT}, s: 0 (curves 1), 20 (2), 40 (3), 60 (4)

Table 1. The determined defect parameters in samples n–GaAs and n–6H–SiC

Sample	t_{MWT}, s	Level	$(E_c - E_t)$, eV	σ_n, cm^2 [a]	R_{cur}, m	ξ_{cur}
SIC1	0	ESC1	0.33 ± 0.01	$(7 \pm 4) \cdot 10^{-18}$	∞	0
	20	ESC1	0.33 ± 0.01	$(5 \pm 3) \cdot 10^{-19}$	170.2	$8.7 \cdot 10^{-7}$
	40	ESC2	0.26 ± 0.01	$(2 \pm 1) \cdot 10^{-19}$		
	80		weak signal			-
SIC2	0	ESC1	0.33 ± 0.01	$(7 \pm 4) \cdot 10^{-18}$	> 2000	$< 1.2 \cdot 10^{-7}$
	20	ESC1	0.33 ± 0.01	$(5 \pm 3) \cdot 10^{-19}$	171.9	$1.4 \cdot 10^{-6}$
SIC3	0	ESC1	0.34 ± 0.02	$(3 \pm 2) \cdot 10^{-18}$	3.8	$6.1 \cdot 10^{-5}$
	20	ESC2	0.29 ± 0.01	$(5 \pm 3) \cdot 10^{-19}$	5.5	$4.2 \cdot 10^{-5}$
	40	ESC2	0.26 ± 0.01	$(10 \pm 7) \cdot 10^{-20}$		
	80	ESC2	0.23 ± 0.01	$(6 \pm 4) \cdot 10^{-20}$		-
GAS1	0	EGA1	0.32 ± 0.02	$(3 \pm 2) \cdot 10^{-17}$	-53.8	$-2.8 \cdot 10^{-6}$
	20	EGA1	0.31 ± 0.01	$(2 \pm 1) \cdot 10^{-17}$	22.9	$6.5 \cdot 10^{-6}$
	40		weak signal			-
GAS2	0	EGA1	0.32 ± 0.01	$(4 \pm 2) \cdot 10^{-17}$	17.2	$8.7 \cdot 10^{-6}$
	20	EGA2	0.28 ± 0.01	$(5 \pm 2) \cdot 10^{-18}$	14.7	$1.0 \cdot 10^{-5}$
	40		weak signal			
GAT	0	EGA3	0.49 ± 0.02	$(5 \pm 3) \cdot 10^{-14}$		
	20	EGA4	0.40 ± 0.02	$(2 \pm 1) \cdot 10^{-15}$		
GAE1	0	EGA5	0.24 ± 0.01	$(2 \pm 1) \cdot 10^{-18}$		
	60	EGA2	0.29 ± 0.01	$(10 \pm 6) \cdot 10^{-18}$		
GAE2	0	EGA5	0.25 ± 0.01	$(2 \pm 1) \cdot 10^{-18}$		
	60	EGA2	0.30 ± 0.01	$(2 \pm 1) \cdot 10^{-17}$		
GAE3	0	EGA6	0.43 ± 0.01	$(8 \pm 5) \cdot 10^{-17}$		-
	60	EGA6	0.46 ± 0.02	$(7 \pm 4) \cdot 10^{-16}$		
GAB1	0	EGA4	0.39 ± 0.01	$(10 \pm 7) \cdot 10^{-18}$		
	20	EGA4	0.39 ± 0.01	$(4 \pm 2) \cdot 10^{-17}$		
	40	EGA6	0.43 ± 0.02	$(10 \pm 6) \cdot 10^{-17}$		
GAB2	0	EGA4	0.40 ± 0.01	$(10 \pm 6) \cdot 10^{-17}$		
	20	EGA4	0.41 ± 0.01	$(10 \pm 6) \cdot 10^{-17}$		
	40	EGA6	0.45 ± 0.02	$(4 \pm 2) \cdot 10^{-16}$		

[a] at $T = 300$ K for SIC, GA, GAE and at $T = 340$ K for GAB

iv) The irradiation dose required to essentially change the parameters of the centers in the epitaxial structures was higher than that required for single-crystal samples. In particular, table 1 provides data for the GA and GAB series samples after 20 s of MWT which supports this fact. Notably, the doping levels of the GAB and GAE substrates were the same as those of samples GAS1 and GAT, and the doping level of the GAB epitaxial layer was similar to that of GAS2. In addition, GAB, GAE, and GAT contain the same doping impurities. Thus, the observed differences were determined by the structure of the samples but not by the difference in their conductivities.
v) The characteristics of changes in single-crystal wafers and epitaxial structures are opposite: for SIC, GAS, GAT, σ_n and $(E_c - E_t)$ were found to decrease after MWT, while for GAE and GAB, both parameters increased.

We now consider the possible configurations of the centers discovered in the structures under study. For this purpose, we should consider that the reported data for the main trap parameters vary over a wide range; in particular, the difference between the values of capture cross sections can be as large as four orders of magnitude [29]. One of the possible reasons for such a large spread is the essential dependence of the thermal charge emission speed on the electric field strength [30, 31] caused by a) decrease in ionization energy due to the Pool–Frenkel effect or, for example, Coulombic interactions of centers [32] and b) change in the σ_n value [33]. As a rule, the change in $(E_c - E_t)$ comprises several tens of meV, and the change in the capture cross-section reaches several orders of magnitude. For instance, according to Bourgoin and Angelis [33], at room temperature, σ_n for the $EL2$ center in GaAs decreases 200 times at an intensity of 10^5 V/cm. Consequently, the different methods used to investigate defects yield different parameters for the same centers. For example, from reviews on various traps in gallium arsenide, we can compare the data obtained by deep-level transient spectroscopy [34] and thermally stimulated currents [29]. Data were obtained for defects with closely located levels and very different capture cross section values. Generalizing the above-mentioned, we should note that it is the energy location of traps that we shall be oriented towards in our research.

The position of the ESC1 level ($E_c - (0.33 - 0.34)$ eV) observed in the initial crystals of silicon carbide can be compared with the position of the S–center ($E_c - 0.35$ eV) [35, 36, 37], EK–center ($E_c - 0.34$ eV) [38], or $(-/+)$ level center $E1$ ($E_c - 0.34$ eV) [35]. S–center is responsible for non-radiative recombination, and in $6H$–SiC it is a self-interstitial defect [35]). According to the results reported in [36, 37], the S–center and R–center ($E_c - 1.27$ eV) are associated with two different charge states of one and the same defect, whereas according to Lebedev *et al* . [39], the R–center is a divacancy $V_{Si}V_C$. It should be noted that a divacancy is a typical defect in $6H$–SiC [40, 20]. On the other hand, the level $E_c - 0.39$ eV is more often associated with center $E1$ [21, 41]. Thus, in our opinion, ESC1 level is related to complex $V_{Si}V_C$.

After the MWT, the position of the level responsible for TAV generation in SiC shifted to $E_c - (0.26 - 0.29)$ eV (level ESC2). And this situation is also ambiguous: closely located are donor level $(0/+)$ of center $E1$ ($E_c - (0.27 - 0.28)$ eV [42], $E_c - 0.26$ eV [21, 41]) and center $X1$ ($E_c - 0.3$ eV [43]). The authors of the latter publication reported the essential dependence of $X1$ concentration on crystal structural perfection. They stressed that this center was not identical to that of center $E1$. In turn, level $E1$ has been identified as the center of the negative correlation energy [43, 21] and dominating intrinsic point defect in n–type $6H$–SiC [44]. According to Refs. [44, 21], $E1$ is related to carbon vacancy. Considering the difference between the $X1$ and ESC2 energy locations, the configuration V_C was associated with the ESC2 level.

The data for every level revealed for gallium arsenide are listed in table 2. The presented data show that the centers are associated with intrinsic vacancy-related defects.

Several factors caused the trap parameters to change. They are as follows.
i) Transformation of the defect complex due to decay, involvement of additional components, change in the distance between defect components, etc.
ii) Defect recharging.
iii) Changes in the trap environment, which can result, for instance, in the modified strength of the electric field around the defect.
iv) An increase in the concentration of a given type of defect; for instance, the change in ionization energy was reported [32] to be proportional to the cubic root of the defect concentration.

Analysis of the observed phenomena should consider the probable mechanisms of the impact of microwave radiation on the crystals. First, the effect of the temperature increase should be analyzed. It is believed that the structural modification in the MWT result is mostly caused by the change in the defect charge state and elastic stress fields arising in instantly heated defect regions. However, these processes are known to intensify with increasing free charge carrier concentrations [6], whereas in our case, the effects weaken with the concentration increase (samples GAS1 and GAS2). Moreover, the applied irradiation mode did not imply long-term continuous exposure to MW

Table 2. Data reported for the levels close to detected levels

$(E_c - E_t)$, eV	σ_n, cm^2	configuration	method[a]	epi–structure	Reference
		EGA1, $(E_c - E_t) = (0.31 - 0.32)$ eV			
0.33	-	complex with V_{As}	DLTS	no	[45]
0.33	-	-	DLTS	no	[46]
$0.31 - 0.33$	-	V_{As}	LDA	no	[47]
0.33	$1 \cdot 10^{-17}$	-	TSC	no	[29]
0.323	$1 \cdot 10^{-14}$	-	DLTS	yes	[48]
0.334	$2 \cdot 10^{-15}$		DLTS	yes	[48]
0.35	-	complex with V_{As}	PA	no	[49]
$0.315 - 0.325$	$3 \cdot 10^{-17}$	-	TSC	no	[50]
0.33	-	-	TSC	no	[51]
$0.30 - 0.33$	-	-	DLTS	no	[52]
		EGA2, $(E_c - E_t) = (0.28 - 0.30)$ eV			
0.28	$5 \cdot 10^{-18}$	$V_{As}As_i$	TSC	no	[29]
0.26	$3.5 \cdot 10^{-15}$	-	DLTS	yes	[48]
0.30	-	intrinsic	DLTS	no	[53]
0.284	$1 \cdot 10^{-17}$	-	TSC	no	[50]
0.28	-	intrinsic	TP	no	[54]
0.28	$8 \cdot 10^{-15}$	-	DLTS	yes	[55]
0.30	-	complex with Te	DLTS	no	[56]
0.30	$6 \cdot 10^{-15}$	$V_{As}As_i$	DLTS	no	[57]
		EGA3, $(E_c - E_t) = 0.49$ eV			
0.50	-	Sb_{Ga}	DLTS	no	[58]
0.48	$4 \cdot 10^{-16}$	As_{Ga}^{++}	TSC	no	[29]
0.485	$2 \cdot 10^{-16}$	-	TSC	no	[50]
0.48	-	impurity	TP	no	[54]
0.49	$2 \cdot 10^{-13}$	impurity+V_{As}	DLTS	yes	[59]
0.48	$3 \cdot 10^{-13}$	-	DLTS	no	[52]
0.50	$1 \cdot 10^{-15}$	V_{As}, $V_{Ga}Ga_iV_{As}$	DLTS	no	[57]
		EGA4, $(E_c - E_t) = (0.39 - 0.41)$ eV			
0.42	-	-	DLTS	no	[46]
0.41	-	$V_{Ga}V_{As}$	DLTS	no	[58]
0.39	-	$V_{Ga}Ga_{As}$	TSC	no	[60]
0.41	$2 \cdot 10^{-13}$	-	DLTS	yes	[34]
0.40	-	-	SCRC	yes	[61]
0.37	$2 \cdot 10^{-14}$	-	DLTS	yes	[62]
0.40	-	$V_{Ga}Ga_{As}$	DLTS	no	[63]
0.387	$2 \cdot 10^{-14}$	-	DLTS	yes	[48]
		EGA5, $(E_c - E_t) = (0.24 - 0.25)$ eV			
0.23	-	-	DLTS	no	[46]
0.23	$2 \cdot 10^{-17}$	-	TSC	no	[29]
$0.22 - 0.25$	$8 \cdot 10^{-19}$	-	TSC	no	[64]
0.26	-	complex with V_{Ga}	TSC	no	[60]
0.24	-	-	TSC	no	[51]
0.23	-	intrinsic	TP	no	[54]
0.23	-	$V_{Ga}V_{As}$	DLTS	no	[65]
0.23	$1 \cdot 10^{-14}$	$V_{Ga}V_{As}$	DLTS	no	[34]
0.23	$7 \cdot 10^{-15}$	-	DLTS	yes	[55]
0.236	$1 \cdot 10^{-16}$	complex with V_{As}	DLTS	yes	[59]
0.258	$4 \cdot 10^{-16}$	-	DLTS	yes	[48]
		EGA6, $(E_c - E_t) = (0.43 - 0.46)$ eV			
0.44	$1 \cdot 10^{-14}$	$V_{As}As_i$, V_{As}	TSC	no	[29]
0.44	$9 \cdot 10^{-15}$	-	TSC	no	[50]
0.43	$7 \cdot 10^{-16}$	intrinsic	DLTS	yes	[66] [34]
0.44	$2 \cdot 10^{-15}$	complex with V_{As}	DLTS	yes	[67]

[a] DLTS — deep level transient spectroscopy; TSC — thermally stimulated current; LDA — local density approximation; PA — positron annihilation techniques; TP — photoinduced transient spectroscopy; SCLC — space charge limited current

oscillations, which reduced the overall heating of the structure. However, numerous studies have shown that the observed effects of MWT cannot be explained only by the mechanisms of fast annealing; therefore, non-thermal factors should also be considered. In recent research, more attention has been paid to the non-thermal mechanisms of MWT action (see, for example, [68] and the references it contains), which cause dislocation generation and result in smaller clusters of point defects in semiconductor wafers [69] or even trigger recrystallization processes [68]. Possible non-thermal processes causing changes in the structural characteristics of binary semiconductors have been reported in [69]. In particular, the processes of dislocation oscillations under the action of an electric field were analyzed, and the decorating impurities were found to influence the behavior of the dislocation segments. On the one hand, the available impurities decrease the resonance frequency of oscillations and provide the presence of electric charge, on the other hand, at high oscillation amplitudes they can escape the dislocation, which causes new chemical defects to arise. In turn, the point defects can perform superhigh-frequency oscillations and diffuse as a result of the MWT.

The observed modifications of deep-level parameters are the result of the above-mentioned structural reconstruction in semiconductor near-surface regions owing to the MWT. The results of X–ray investigations show that MWT increases the convexity of single-crystal samples, which indicates the aggregation of interstitial defects in the near-surface layer, particularly because of the generation of separate dislocations [11, 19]. The defect accumulation effect caused by the MWT in the near-surface region was reported in [11, 18]. To a certain extent, only the SIC3 sample was excluded; however in this case, a rather strong deformation of the near-surface region was also observed prior to irradiation. Researchers have reported [9, 10, 11, 12, 13] that in this stressed state, MWT causes redistribution as well as certain weakening of elastic deformations, which is what occurs in SIC3. The profilometry data correlated with X–ray measurements. Structural investigations show that in the initial GaAs samples, the density of dislocations has a W-like distribution over the plate area; the dislocation density over the plate diameter varied from $2{\cdot}10^4$ cm^{-2} to $2\cdot10^5$ cm^{-2}. This inhomogeneity in the dislocation density distribution is evidence of considerably strong elastic deformation in the sample.

The analysis showed that the ESC1 and ESC2 centers are complexes of carbon vacancies, EGA1 is associated with V_{As}, and EGA3 — with V_{As} or $V_{Ga}Ga_iV_{As}$ complexes. The MWT stimulates the diffusion of point defects, which are mostly intrinsic interstitial atoms, resulting in trap modifications. The ESC1 center in silicon carbide transforms into ESC2 under the influence of closely located interstitial silicon:

$$V_{Si}\ V_C + Si_i \rightarrow V_C\,.$$

Further modification of the ESC2 parameters in SIC3 is caused by the enhanced electric field of the dislocation. In the GAS2 samples at $t_{MWT} = 20$ s, the V_{As} transformed into complex $V_{As}As_i$ (EGA2 center) because of the increased number of interstitial atoms in the near-surface layer:

$$V_{As} + As_i \rightarrow V_{As}\ As_i\,.$$

A similar process in GAS1 is more complicated because of its higher charge carrier concentration. It has been reported [7] that with a growth in resistance, the depth of microwave penetration increases, and thus, the volume from which defect gettering begins in the near-surface layer grows as well. In addition, the cause of the weak (in comparison with GAS2) influence of MWT on trap parameters in GAS1 is the absence of pressure stresses, which intensifies the MWT-simulated complex formation process in the system's intrinsic defects. This is supported by data for silicon carbide single crystals. In the GAT sample, which is also characterized by a high concentration of free electrons, the transformation of EGA3 to EGA4 ($V_{Ga}Ga_{As}$ complex) occurs in the reaction described in [60]:

$$V_{Ga}\ Ga_i\ V_{As} \rightarrow Ga_{Ga}\ V_{As} \rightarrow Ga_{As}\ V_{Ga}$$

Accumulation of a large number of interstitial atoms in the near-surface layer at high doses of radiation ($t_{MWT} \approx 40$ s for gallium arsenide and $t_{MWT} > 80$ s for silicon carbide) causes complete annihilation of vacancies (or transformation into antisite defects, whose levels are filled in the crystals with electron conductivity); therefore, the TAV signal disappears (samples GAS1, GAS2, SIC1):

$$\text{SiC} \quad : V_{Si}\ V_{Si} + Si_i + Si_i \rightarrow 0\,;$$

$$\text{GaAs} : V_{As} + As_i \rightarrow 0\,; \quad V_{As} + Ga_i \rightarrow Ga_{As}\,.$$

It is believed [27, 25, 24] that the TAV that arises in epitaxial structures is mostly caused by defects located at the epi–layer and substrate interface. This difference in the deep-level location is the cause of the difference between the dose-dependent modification of the defect parameters in the epitaxial and single-crystal samples.

In epitaxial structures n–n^+–GaAs and n–n^+–n^{++}–GaAs, MWT induced increase of curvature radius reported in [11, 19] is the result of forming single dislocations and their further propagation deep into the structure along the glide planes. As a result, the strength of both the electric and stress fields changes, which causes defect transformation and, thus, the shift

of the respective deep levels. As shown in table 2, EGA5 and EGA6 levels were associated with the complexes $V_{Ga}V_{As}$ and $V_{As}As_i$, respectively. Traps such as EGA2 and EGA4 have also been previously found in epi-structures [48, 55, 34, 61, 62, 66, 67]. The observed MWT-stimulated transformations are caused by an increasing number of interstitial atoms, which are described by the following reactions:

$$V_{Ga}\ V_{As} + Ga_i + As_i \rightarrow V_{As}\ As_i$$

for GAE1 and GAE2 and

$$V_{Ga}\ Ga_{As} + As_i \rightarrow Ga_{Ga}\ V_{As} + As_i \rightarrow V_{As}\ As_i$$

for GAB1 and GAB2. The increase in activation energy EGA6 in sample GAE3 is probably caused by the change in Coulombic interaction of interstitial–vacancy complexes, which is due to a decrease in their concentration, while the growth of capture cross section EGA4 in GAB1 at $t_{MWT} = 20$ s and EGA6 in GAE3 are associated with the growth of the electric field strength caused by charged dislocations.

4. Conclusion

The influence of microwave radiation on the parameters of point defects (cross section of electron capture and energy levels in the gap) was studied experimentally in single crystals of n–6H-SiC and n–GaAs, as well as in gallium arsenide epitaxial structures. The investigation showed that the traps available in the near-surface layer are associated with intrinsic vacancy-related defects. The microwave radiation-induced change in the trap energy level and capture cross section was caused by the growing number of interstitial atoms in the near-surface layer. The radiation-induced process involving the transformation of defect complexes intensifies under stress conditions. Thus microwave processing can be an effective tool of defect engineering.

Data Availability Statement

The data that support the findings of this study are available from the corresponding author upon reasonable request.

References

[1] Kozlovskii V V, Kozlov V A and Lomasov V N 2000 *Semiconductors* **34**(2) 123–140

[2] Schrimpf R D and Fleetwood D M 2004 *Radiation Effects and Soft Errors in Integrated Circuits and Electronic Devices* (World Scientific) ISBN 981-238-940-7

[3] Kabiraj D and Ghosh S 2011 *J. Appl. Phys.* **109** 033701

[4] Olikh O Y, Gorb A M, Chupryna R G and Pristay-Fenenkov O V 2018 *J. Appl. Phys.* **123** 161573

[5] Olikh O and Pinchuk T 2006 *Tech. Phys. Lett.* **32** 517–519

[6] Kitchen H J, Vallance S R, Kennedy J L, Tapia-Ruiz N, Carassiti L, Harrison A, Whittaker A G, Drysdale T D, Kingman S W and Gregory D H 2014 *Chem. Rev.* **114** 1170–1206

[7] Zohm H, Kasper E, Mehringer P and Müller G 2000 *Microelectron. Eng.* **54** 247–253

[8] Bhunia S and Bose D 1998 *J. Cryst. Growth* **186** 535–542

[9] Bacherikov Y Y, Konakova R V, Kocherov A N, Lytvyn P M, Lytvyn O S, Okhrimenko O B and Svetlichnyi A M 2003 *Technical Physics* **48**(5) 598–601

[10] Pashkov V, Perevoshchikov V and Skupov V 1994 *Pis'ma v zhurnal tekhnicheskoy fiziki* **20**(8) 14–18 (in Russian)

[11] Boltovets N S, Kamalov A B, Kolyadina E Y, Konakova R V, Lytvyn P M, Lytvyn O S, Matveeva L A, Milenin V V and Rengevych O E 2002 *Technical Physics Letters* **28**(2) 154–156

[12] Milenin V, Konakova R, Statov V, Sklyarevich V, Tkhorik Y, Filatov M and Shevelev M 1994 *Pis'ma v zhurnal tekhnicheskoy fiziki* **20**(4) 32–36 (in Russian)

[13] Belyaev A, Venger E, Ermolovich I, Konakova R, Lytvyn P, Milenin V, Prokopenko I, Svechnikov G, Soloviev E and Fedorenko L 2002 *Effect of microwave and laser radiations on the parameters of semiconductor structures* (Kyiv: Intac)

[14] Ashkinadze B, Cohen E, Ron A, Linder E and Pfeiffer L 1996 *Solid-State Electron.* **40** 561–565 ISSN 0038-1101

[15] Ermolovich I B, Venger E F, Konakova R V, Milenin V V, Svechnikov S V and Sheveljev M V 1998 *Proc. SPIE* **3359** 265–272

[16] Belyayev A, Belyayev A, Yermolovich I, Komirenko S, Konakova R, Lyapin V, Milenin V, Solov'ev E and Shevelev M 1998 *Technical Physics* **43** 1445–1449

[17] Bacherikov Y, Konakova R, Milenin V, Okhrimenko O, Svetlichnyi A and Polyakov V 2008 *Semiconductors* **42**(7) 868–872

[18] Zayats N S, Konakova R V, Milenin V V, Milenin G V, Red'ko R A and Red'ko S N 2015 *Technical Physics* **60**(3) 432–436

[19] Belyayev A, Sachenko A, Boltovets N, Ivanov V, Konakova R, Kudryk Y, Matveeva L, Milenin V, Novitskii S and Sheremet V 2012 *Semiconductors* **46**(4) 541–544

[20] Davidsson J, Ivády V, Armiento R, Ohshima T, Son N T, Gali A and Abrikosov I A 2019 *Appl. Phys. Lett.* **114** 112107

[21] Wei Y, Tarekegne A T and Ou H 2018 *J. Appl. Phys.* **124** 054901

[22] Pellegrino C, Gagliardi A and Zimmermann C G 2020 *J. Appl. Phys.* **128** 195701

[23] Sobolev M M, Soldatenkov F Y and Danil'chenko V G 2020 *J. Appl. Phys.* **128** 095705

[24] Ostrovskii I V, Saiko S V and Walther H G 1998 *J. Phys. D: Appl. Phys.* **31** 2319–2325

[25] Ostrovskii I and Olikh O 1998 *Solid State Commun.* **107** 341–343 ISSN 0038-1098

[26] Gromashevskii V, Tatyanenko N and Snopok B 2013 *Semiconductors* **47**(4) 579–585

[27] Abbate A, Ostrovskii I V, Han K J, Masini G, Palma F and Das P 1995 *Semicond. Sci. Technol.* **10** 965–969

[28] Godwod K, Nagy A T and Rek Z 1976 *Phys. Status Solidi A* **34** 705–710

[29] Pavlović M, Desnica U V and Gladić J 2000 *J. Appl. Phys.* **88** 4563–4570

[30] Bulyarskii S, Grushko N and Zhukov A 2000 *Semiconductors* **34**(1) 40–44

[31] Makram-Ebeid S and Lannoo M 1982 *Phys. Rev. B* **25**(10) 6406–6424

[32] Stellmacher M, Bisaro R, Galtier P, Nagle J, Khirouni K and Bourgoin J C 2001 *Semicond. Sci. Technol.* **16** 440–446

[33] Bourgoin J C and De Angelis N 2001 *Semicond. Sci.*

Technol. **16** 497–501
[34] Bourgoin J C, von Bardeleben H J and Stiévenard D 1988 *J. Appl. Phys.* **64** R65–R92
[35] Lebedev A A 1999 *Semiconductors* **33**(2) 107–130
[36] Anikin M, Andreyev A, Lebedev A, Pyatko S, Rastegayeva M, Savkina N, Strel'chuk A, Syrkin A and Chelnokov V 1991 *Fizika i tekhnika poluprovodnikov* **25**(2) 328–333 (in Russian)
[37] Anikin M, Zubrilov A, Lebedev A, Strel'chuk A and Cherenkov A 1991 *Fizika i tekhnika poluprovodnikov* **25**(3) 479–486 (in Russian)
[38] Kuznetsov N and Edmond J 1997 *Semiconductors* **31**(10) 1049–1052
[39] Lebedev A, Veinger A, Davydov D, Kozlovskii V, Savkina N and Strel'chuk A 2000 *Semiconductors* **34**(8) 861–866
[40] Baranov P G, Il'in I V, Mokhov E N, Muzafarova M V, Orlinskii S B and Schmidt J 2005 *Journal of Experimental and Theoretical Physics Letters* **82** 441–443
[41] Koizumi A, Markevich V P, Iwamoto N, Sasaki S, Ohshima T, Kojima K, Kimoto T, Uchida K, Nozaki S, Hamilton B and Peaker A R 2013 *Appl. Phys. Lett.* **102** 032104
[42] Hemmingsson C G, Son N T and Janzén E 1999 *Appl. Phys. Lett.* **74** 839–841
[43] Lebedev A, Davydov D, Tregubova A, Bogdanova E, Shcheglov M and Pavlenko M 2001 *Semiconductors* **35**(12) 1372–1374
[44] Sasaki S, Kawahara K, Feng G, Alfieri G and Kimoto T 2011 *J. Appl. Phys.* **109** 013705
[45] Richter T, Kühnel G, Siegel W and Niklas J R 2000 *Semicond. Sci. Technol.* **15** 1039–1044
[46] Neild S T, Skowronski M and Lagowski J 1991 *Appl. Phys. Lett.* **58** 859–861
[47] Schultz P A 2015 *J. Phys.: Condens. Matter* **27** 075801
[48] Yousefi G H, Webb J B, Rousina R and Khanna S M 1995 *J. Electron. Mater.* **24** 15–20
[49] Kuisma S, Saarinen K, Hautojärvi P, Fang Z Q and Look D 1997 *J. Appl. Phys.* **81** 3512–3521
[50] Pavlović M and Desnica U V 1998 *J. Appl. Phys.* **84** 2018–2024
[51] Tomozane M and Nannichi Y 1986 *Japanese Journal of Applied Physics* **25** L273–L275
[52] Lang D V, Cho A Y, Gossard A C, Ilegems M and Wiegmann W 1976 *J. Appl. Phys.* **47** 2558–2564
[53] Stievenard D, Boddaert X and Bourgoin J C 1986 *Phys. Rev. B* **34**(6) 4048–4058
[54] Abele J C, Kremer R E and Blakemore J S 1987 *J. Appl. Phys.* **62** 2432–2438
[55] Mircea A and Mitonneau A 1975 *Applied physics* **8** 15–21
[56] Kol'chenko T and Lomako V 1994 *Fizika i tekhnika poluprovodnikov* **28**(5) 857–860 (in Russian)
[57] Pons D and Bourgoin J C 1985 *J. Phys. C: Solid State Phys.* **18** 3839–3871
[58] Samoylov V A, Yakusheva N A and Prints V Y 1994 *Fizika i tekhnika poluprovodnikov* **28**(9) 1617–1626 (in Russian)
[59] Blood P and Harris J J 1984 *J. Appl. Phys.* **56** 993–1007
[60] Fang Z, Shan L, Schlesinger T and Milnes A 1990 *Materials Science and Engineering: B* **5** 397–408
[61] Ashby A, Roberts G, Ashen D and Mullin J 1976 *Solid State Commun.* **20** 61–63
[62] Fang Z Q, Schlesinger T E and Milnes A G 1987 *J. Appl. Phys.* **61** 5047–5050
[63] Vaytkus Y, Storasta Y, Pintsevichyus A, Pyatrauskas M and Kazhukauskas V 1988 *Litovskiy fizicheskiy sbornik* **28**(6) 744–751 (in Russian)
[64] Lin A L, Omelianovski E and Bube R H 1976 *J. Appl. Phys.* **47** 1852–1858
[65] Morrow R A 1991 *J. Appl. Phys.* **69** 3396–3398
[66] Lefèvre H and Schulz M 1977 *Applied physics* **12** 45–53
[67] Kol'chenko T, Lomako V, Rodionov A and Sveshnikov Y 1989 *Fizika i tekhnika poluprovodnikov* **23**(4) 626–629 (in Russian)
[68] Nozariasbmarz A, Dsouza K and Vashaee D 2018 *Appl. Phys. Lett.* **112** 093103
[69] Ermolovich I, Milenin G, Milenin V, Konakova R and Red'ko R 2007 *Technical Physics* **77**(9) 1173–1177